AIAA JOURNAL
Vol. 31, No. 4, April 1993

Dynamic Analysis and Design of Laminated Composite Beams with Multiple Damping Layers

Mohan D. Rao* and Shulin He†
Michigan Technological University, Houghton, Michigan 49931

This paper describes the formulation of a theory for the prediction of damping and natural frequencies of laminated composite beams with multiple viscoelastic damping layers. The damping layers are constrained (or sandwiched) by anisotropic laminates. The in-plane shear strains of the damping layers and the constraining layers are included in the model. Closed-form solutions for the resonance frequencies and modal loss factors of the composite beam system under simple supports are derived using the energy and Ritz method. A parametric study has been conducted to study the variation of dynamic stiffness and modal loss factor of the system with structural parameters (e.g., the ply orientations of laminas, thickness of the damping layers and the laminates), operating temperature, and damping material properties. The design of composite beams for maximizing the damping capacity is also presented in this paper which includes the determination of operating temperature range corresponding to given structural parameters and finding optimal structural parameters corresponding to given temperature range. Finally, some experimental results are compared with theory for the cases of single and double damping layer beam systems that show good agreement between predicted and measured natural frequencies.

Nomenclature

$C(i)$ = the ith damping layer ($i = 1, \ldots, 2N-1$)
$E_{C(i)}$ = complex elastic modulus of the ith damping layer
$E'_{C(i)}$ = elastic storage modulus of the ith damping layer
$G_{C(i)}$ = complex shear modulus of the ith damping layer
$G'_{C(i)}$ = shear storage modulus of the ith damping layer
$H_{C(i)}$ = thickness of the ith damping layer
H_i = thickness of the ith laminate ($i = 1, \ldots, 2N$)
$k_{i,j}$ = constant element in the coefficient matrix of Eq. (36) ($i,j = 1, \ldots, n$)
L = total length of the composite beam
M = mass per unit length of the composite beam
$2N$ = total number of laminates of the composite beam
N_i = number of layers in the ith laminate
$q(x, t)$ = external load on the composite beam along z direction
$\bar{Q}_{kl}^{(i,j)}$ = element of the transformed reduced stiffness matrix of the jth layer of the ith laminate
T_k = kinetic energy of the composite beam
$t_j^{(i)}$ = thickness of the jth layer of the ith laminate
U_B = total strain energy of all of the laminates
U_C = total strain energy of the damping layers
$U^{(i)}$ = strain energy of the ith laminate
$U_{C(i)}$ = strain energy of the ith damping layer
$u_{C(i)}$ = longitudinal displacement of the ith damping layer
u_i = longitudinal displacement of the ith laminate
W = work done by $q(x, t)$
$w(x, t)$ = transverse displacement of every layer of the composite beam
x = longitudinal coordinate
z = thickness coordinate
$z_c^{(i)}$ = $z_1^{(i)}$ (see Fig. 1)
$z_j^{(i)}$ = z coordinate of the surface close to the xy plane of the jth layer of the ith laminate
$\bar{z}_j^{(i)}$ = z coordinate of the middle surface of the jth layer of the ith laminate
$\gamma_{xy}^{C(i)}$ = in-plane (xy plane) shear strain of the ith damping layer ($i = 1, 2, \ldots, 2N-1$)
$\gamma_{xz}^{C(i)}$ = xz plane shear strain of the ith damping layer ($i = 1, \ldots, 2N-1$)
$\gamma_{xy}^{(i)}$ = in-plane (xy plane) shear strain of the ith laminate ($i = 1, \ldots, 2N$)
$\Delta K_{i,j}$ = cofactor of $k_{i,j}$ in the coefficient matrix of Eq. (36)
δ = variational operator
$\epsilon_x^{C(i)}$ = longitudinal strain of the ith damping layer
$\epsilon_x^{(i)}$ = longitudinal strain of the ith laminate
η = modal loss factor of the composite beam
$\eta_{C(i)}$ = shear or extensional loss factor of the ith damping material
ω = flexural vibration frequency (rad/s)
ω_γ = resonance frequency of the composite beam
$\theta^{(i,j)}$ = angle between the fiber direction of the jth layer of the ith laminate and x axis
$\rho_{C(i)}$ = density of the ith damping material
ρ_i = density of the ith lamina material
$\sigma_x^{(i,j)}$ = x directional normal stress component of the jth layer of the ith laminate
$\sigma_y^{(i,j)}$ = y directional normal stress component of the jth layer of the ith laminate
$\tau_{xy}^{(i,j)}$ = xy plane shear stress component of the jth layer of the ith laminate

Received April 4, 1992; revision received Aug. 27, 1992; accepted for publication Sept. 1, 1992.

*Assistant Professor, Mechanical Engineering-Engineering Mechanics Department.
†Graduate Research Assistant, Mechanical Engineering-Engineering Mechanics Department.

Introduction

THE dynamic analysis of sandwich beams and plates has been one of the central topics of investigation in the field of noise and vibration control for over thirty years. The pioneering work in analyzing the damping behavior of a primary beam (structure) with a viscoelastic damping layer and a constraining beam added on to it was done by Ross et al.[1] Since then, many papers have appeared in the literature for analyzing sandwich structures including damping of bonded structures incorporating viscoelastic damping layers,[2-8] and structures with multiple damping layers.[9-11] The cited analyses for multiple damping layer, however, are valid only for the case of elastic and isotropic face plates and constraining layers.

In recent years, research has been concentrated on the analysis of anisotropic laminated damped beams and plates. When the two face plates are composite laminates, the previous models developed for isotropic face plates are not accurate.

Tujimota et al.[10] used both experimental work and theory for sandwich beams with isotropic face plates to study the damping characteristics of multilayer composite sandwich plates. In some cases, especially for the anisotropic case, the experimental results diverged from the numerical results. Part of the reason for this discrepancy was believed to be the anisotropic nature of each of the face plates. Mukhopadhyay and Kingsbury[11] pointed out that when the sandwich plate undergoes flexural deformation, the anisotropic facings will not only deform under normal strain, but also undergo shear deformation in their own planes, because of the coupling between the bending and extensional motion, and the coupling between shear and extensional deformation. Unlike conventional sandwich beams with isotropic facings, the additional in-plane shear deformation in the face plates will influence the in-plane shear deformation of the damping layer. Also, when the facings are made of composite materials, the material damping of the face plates needs to be included in the analysis. A comprehensive model to predict the damping of composite laminated plates with a single damping layer has been developed by Barrett.[12]

In this paper, the authors have developed a comprehensive, yet simple model to study the dynamic behavior of multidamping layer composite beams with anisotropic laminated constraining layers. The dominating factors that affect the damping efficiency of the composite beam are believed to be the shear deformation of the damping layers in both the xz plane and the xy plane (see Fig. 1a), and are considered in the current analysis. Numerical examples are presented in the paper to show the effects of structural parameters, operating temperature, and different damping materials on the system dynamic parameters. The design procedure of composite beams is also illustrated using the preceding numerical results for various cases.

Theory

The multidamping layer composite beam is shown in Fig. 1a. For determining the strain fields of the composite beam, the extensional and the in-plane shear strains in the constraining layers and in the damping layers are included. The xz plane shear strains in the constraining layers are also considered.

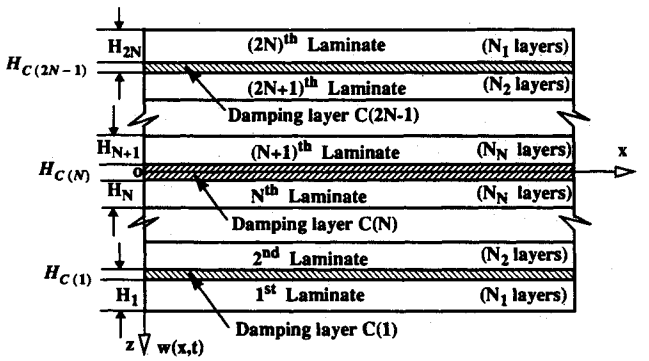

a) Multidamping layer composite beam system

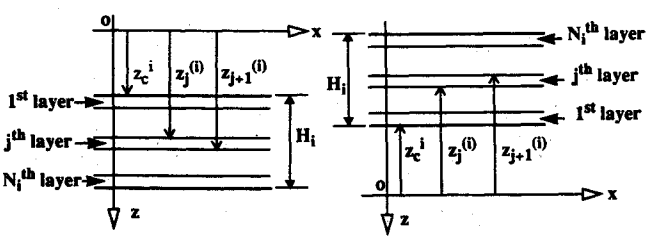

b) ith laminated beam located in positive z axis

c) ith laminated beam located in negative z axis

Fig. 1 Configuration and coordinates of the multidamping layer composite beam.

The following basic assumptions are made in the current analysis:

1) The composite beam has a unit width, $(2N-1)$ damping layers and $2N$ laminates (i.e., constraining layers). It is simply supported and is symmetric with respect to the xy plane.

2) The shear strain $\gamma_{xy}^{(i)}$ is constant through the thickness of the ith laminate and $\gamma_{xz}^{C(i)}$ is also constant through the thickness of the ith damping layer; but $\gamma_{xy}^{C(i)}$ varies linearly through the thickness of the ith damping layer.

3) Normal strain $\epsilon_x^{(i)}$ varies linearly through the thickness of the ith laminate.

4) Transverse displacement $w(x, t)$ is the same for every layer of the composite beam, and only the transverse directional inertia of the composite beam is included.

5) The normal stress components σ_y and σ_z of each layer are neglected.

In addition, the longitudinal displacement of each damping layer is approximated to be constant through its thickness for simplifying the calculation of the longitudinal strain energy of the damping layer. Because of the symmetry of the composite beam with respect to xy plane, we have

$$H_{(2N+1)-i} = H_i,\ \gamma_{xy}^{(2N+1-i)} = -\gamma_{xy}^{(i)}, \qquad i = 1, \ldots, N$$

and

$$H_{C(2N-i)} = H_{C(i)},\ \gamma_{xz}^{C(2N-i)} = \gamma_{xz}^{C(i)}, \qquad i = 1, \ldots, N-1$$

Strain Energy Analysis of the Composite Beam

When the normal stresses of each layer in the y and z directions are neglected, only the displacement along the x direction (axial direction) of the beam needs to be defined. The longitudinal displacement field of the composite beam can be described as follows.

For the ith laminated beam

$$u_i(z, x, t) = z\frac{\partial w}{\partial x} - \left(\frac{H_{C(N)}}{2}\gamma_{xz}^{C(N)} + \sum_{k=i}^{N-1} H_{C(k)}\gamma_{xz}^{C(k)}\right)$$

$$i = 1, \ldots, N \tag{1}$$

where

$$z_c^i \le z \le z_c^i + H_i \tag{2a}$$

$$\pm z_c^i = \frac{1}{2}H_{C(N)} + \sum_{k=i}^{N-1} H_{C(k)} + \sum_{k=i+1}^{N} H_k$$

and

$$u_i(z, x, t) = -u_{2N+1-i}(-z, x, t) \tag{2b}$$

$$i = N+1, \ldots, 2N$$

For damping layer C_i, we have

$$u_{C_i}(x, t) = \tfrac{1}{2}[u_i|_{z=(z_c^i - H_{C(i)})} + u_{i+1}|_{z=z_c^i}$$

that is,

$$u_{C(i)}(x, t) = (z_c^i - \tfrac{1}{2}H_{C(i)})\frac{\partial w}{\partial x} - \left[\tfrac{1}{2}(H_{C(i)}\gamma_{xz}^{C(i)} + H_{C(N)}\gamma_{xz}^{C(N)}) + \sum_{k=i+1}^{N-1} H_{C(k)}\gamma_{xz}^{C(k)}\right] \qquad i = 1, 2, \ldots, N-1 \tag{3}$$

$$u_{C(i)}(x, t) = -u_{C(2N-i)}(x, t) \tag{4}$$

$$i = N+1, \ldots, 2N-1$$

Through the given displacement description, the longitudinal and shear strain fields of the composite beam can be determined. For the ith laminate, we have

$$\epsilon_x^{(i)}(z, x, t) = z\frac{\partial^2 w}{\partial x^2} - \left(\frac{H_{C(N)}}{2}\frac{\partial \gamma_{xz}^{C(N)}}{\partial x} + \sum_{k=i}^{N-1} H_{C(k)}\frac{\partial \gamma_{xz}^{C(k)}}{\partial x}\right) \tag{5}$$

$$z_c^i \le z \le z_c^i + H_i$$

$$\gamma_{xy}^{(i)}(x, t) = \gamma_{xy}^{(i)}(x, t) \tag{6}$$

for $i = 1, \ldots, N$, and

$$\epsilon_x^{(i)}(z, x, t) = -\epsilon_x^{(2N+1-i)}(-z, x, t) \tag{7}$$

$$\gamma_{xy}^{(i)}(x, t) = -\gamma_{xy}^{(2N+1-i)}(x, t) \tag{8}$$

for $i = N+1, \ldots, 2N$.

The strain components $\epsilon_x^{C(i)}$, $\gamma_{xy}^{C(i)}$, and $\gamma_{xz}^{C(i)}$ of damping layer $C(i)$ can be shown to be

$$\epsilon_x^{C(i)}(x, t) = \left(z_i - \frac{H_{C(i)}}{2}\right)\frac{\partial^2 w}{\partial x^2} - \left[\frac{H_{C(i)}}{2}\frac{\partial \gamma_{xz}^{C(i)}}{\partial x} + \frac{H_{C(N)}}{2}\frac{\partial \gamma_{xz}^{C(N)}}{\partial x} + \sum_{k=i+1}^{N-1} H_{C(k)}\frac{\partial \gamma_{xz}^{C(k)}}{\partial x}\right] \tag{9}$$

$$\gamma_{xy}^{C(i)}(z, x, t) = \gamma_{xy}^{(i+1)} + \frac{1}{H_{C_i}}[z - (z_c^i - H_{C(i)})][\gamma_{xy}^{(i)} - \gamma_{xy}^{(i+1)}] \tag{10}$$

$$z_c^i - H_{C_i} \le z \le z_c^i$$

$$\gamma_{xz}^{C(i)}(x, t) = \gamma_{xz}^{C(i)}(x, t) \tag{11}$$

for $i = 1, 2, \ldots, N-1$, and

$$\epsilon_x^{C(i)}(x, t) = -\epsilon_x^{C(2N-i)}(x, t) \tag{12}$$

$$\gamma_{xy}^{C(i)}(-z, x, t) = -\gamma_{xy}^{C(2N-i)}(z, x, t) \tag{13}$$

$$\gamma_{xz}^{C(i)}[-(z, x), t] = \gamma_{xz}^{C(2N-i)}(z, x, t) \tag{14}$$

for $i = N+1, \ldots, 2N-1$.

As for the damping layer $C(N)$, since the middle surface of this layer is the neutral surface of the composite beam, $\epsilon_x^{C(N)}$ is approximated to be zero. The shear strains of this layer are given by

$$\gamma_{xz}^{C(N)}(x, t) = \gamma_{xz}^{C(N)}(x, t) \tag{15}$$

$$\gamma_{xy}^{C(N)}(z, x, t) = \frac{2z}{H_{C(N)}}\gamma_{xy}^{(N)}(x, t) \tag{16}$$

$$-\tfrac{1}{2}H_{C(N)} \le z \le \tfrac{1}{2}H_{C(N)}$$

Now consider the jth layer of the ith laminate. Figures 1b and 1c show the coordinates of the ith laminate in the global coordinate system. We can show that

$$t_j^{(i)} = |z_{j+1}^{(i)} - z_j^{(i)}| \quad \text{and} \quad \bar{z}_j^{(i)} = (z_j^{(j)} + z_{j+1}^{(i)})/2 \tag{17}$$

Applying the stress-strain formula from Ref. 13, we have

$$\begin{bmatrix} \sigma_x^{(i,j)} \\ \sigma_y^{(i,j)} \\ \tau_{xy}^{(i,j)} \end{bmatrix} = \begin{bmatrix} \bar{Q}_{11}^{(i,j)} & \bar{Q}_{12}^{(i,j)} & \bar{Q}_{16}^{(i,j)} \\ \bar{Q}_{12}^{(i,j)} & \bar{Q}_{22}^{(i,j)} & \bar{Q}_{26}^{(i,j)} \\ \bar{Q}_{16}^{(i,j)} & \bar{Q}_{26}^{(i,j)} & \bar{Q}_{66}^{(i,j)} \end{bmatrix} \begin{bmatrix} \epsilon_x^{(i,j)} \\ \epsilon_y^{(i,j)} \\ \epsilon_{xy}^{(i,j)} \end{bmatrix} \tag{18}$$

Since, here, $\sigma_y^{(i,j)} = 0$, the stress-strain relation (18) can be reduced to

$$\sigma_x^{(i,j)} = [\bar{Q}_{11}(i, j)]\epsilon_x^{(i,j)} + [\bar{Q}_{16}(i, j)]\gamma_{xy}^{(i,j)} \tag{19}$$

$$\tau_{xy}^{(i,j)} = [\bar{Q}_{16}(i, j)]\epsilon_x^{(i,j)} + [\bar{Q}_{66}(i, j)]\gamma_{xy}^{(i,j)} \tag{20}$$

where $\bar{Q}_{16}(i, j) = \bar{Q}_{16}^{(i,j)} - (\bar{Q}_{12}^{(i,j)})^2/\bar{Q}_{26}^{(i,j)}$, $\bar{Q}_{16}(i, j) = \bar{Q}_{16}^{(i,j)} - (\bar{Q}_{22}^{(i,j)}\bar{Q}_{26}^{(i,j)})/\bar{Q}_{22}^{(i,j)}$, and $\bar{Q}_{66}(i, j) = \bar{Q}_{66}^{(i,j)} - (\bar{Q}_{26}^{(i,j)})^2/\bar{Q}_{22}^{(i,j)}$.

The strain energy density of the jth layer is given by

$$U_0^{(i,j)} = \tfrac{1}{2}[\bar{Q}_{11}(i, j)](\epsilon_x^{(i,j)})^2 + \tfrac{1}{2}[\bar{Q}_{66}(i, j)](\gamma_{xy}^{(i,j)})^2 + \bar{Q}_{16}(i, j)\epsilon_x^{(i,j)}\gamma_{xy}^{(i,j)} \tag{21}$$

Then, the strain energy of the ith laminated beam can be integrated by

$$U^{(i)} = \int_0^L \left[\sum_{j=i}^{N_i}\left(\int_{z_j^{(i)}}^{z_j^{(i)}+1} U_0^{(i,j)}\, dz\right)\right] dx \tag{22}$$

for unit width, in which $z_1^{(i)} = z_c^i$ and $z_{N_i+1}^{(i)} = z_c^i + H_i$. The integration of Eq. (22) gives

$$U^{(i)} = \int_0^L \sum_{j=1}^{N_i} t_j^{(i)}\left\{\tfrac{1}{2}\bar{Q}_{66}(i, j)(\gamma_{xy}^{(i)})^2 + \tfrac{1}{2}\bar{Q}_{11}(i, j)\left[\left(\bar{z}_j^{(i)2} + \frac{(t_j^{(i)})^2}{12}\right)\left(\frac{\partial^2 w}{\partial x^2}\right)^2 - 2\bar{z}_j^{(i)}\left(\frac{H_{C(N)}}{2}\frac{\partial \gamma_{xz}^{C(N)}}{\partial x} + \sum_{k=i}^{N-1} H_{C(k)}\frac{\partial \gamma_{xz}^{C(k)}}{\partial x}\right)\frac{\partial^2 w}{\partial x^2} + \left(\frac{H_{C(N)}}{2}\frac{\partial \gamma_{xz}^{C(N)}}{\partial x} + \sum_{k=i}^{N-1} H_{C(k)}\frac{\partial \gamma_{xz}^{C(k)}}{\partial x}\right)^2\right] - \bar{Q}_{16}(i, j)\gamma_{xy}^{(i)}\left(\frac{H_{C(N)}}{2}\frac{\partial \gamma_{xz}^{C(N)}}{\partial x} + \sum_{k=i}^{N-1} H_{C(k)}\frac{\partial \gamma_{xz}^{C(k)}}{\partial x} - \bar{z}_j^{(i)}\frac{\partial^2 w}{\partial x^2}\right)\right\} dx \tag{23}$$

for $i = 1, 2, \ldots, N$.

Because of the symmetry of the composite beam, we can show that

$$U^{(i)} = U^{(2N+1-i)}, \qquad i = N+1, \ldots, 2N \tag{24}$$

The total strain energy contributed by the constrained layers is given by

$$U_B = 2\sum_{i=1}^{N} U^{(i)} \tag{25}$$

The strain energy in damping layer $C(i)$ $(i = 1, \ldots, N-1)$ can be calculated by

$$U^{C(i)} = \frac{1}{2}\int_0^L \left\{\int_{z_c^{i+1}}^{z_c^i} [E_{C(i)}(\epsilon_x^{C(i)})^2 + G_{C(i)}(\gamma_{xy}^{C(i)})^2 + G_{C(i)}(\gamma_{xz}^{C(i)})^2]\, dz\right\} dx \tag{26}$$

The strain energy of damping layer $C(N)$ is given by

$$U^{C(n)} = \frac{H_{C(N)}G_{C(N)}}{2}\int_0^L \left[(\gamma_{xz}^{C(N)})^2 + \tfrac{1}{3}(\gamma_{xy}^{(N)})^2\right] dx \tag{27}$$

As for the other $N-1$ damping layers, we can show that

$$U^{C(i)} = U^{C(2N-1)} \qquad \text{for} \quad i = N+1, \ldots, 2N-1 \tag{28}$$

Then the total strain energy contributed by the $2N-1$ damping layers is given by

$$U_C = U^{C(N)} + 2\sum_{i=1}^{N-1} U^{C(i)} \tag{29}$$

When only the transverse inertia is included, the kinetic energy of the composite beam is

$$T_k = \frac{1}{2}\int_0^L M\left(\frac{\partial w}{\partial t}\right)^2 dx \tag{30}$$

where

$$M = 2\rho_N H_N + \rho_{C(N)} H_{C(N)} + \sum_{i=1}^{N-1} 2(\rho_i H_i + \rho_{C(i)} H_{C(i)})$$

The work done by $q(x, t)$ is given by

$$W = \int_0^L q(x, t) w(x, t)\, dx \tag{31}$$

Assuming that the energy dissipated in the composite beam is balanced by the work done by the external distribution load $q(x, t)$, the system differential equations of motion can be obtained by the application of the Hamilton's principle which is given by

$$\delta \int_0^{\Delta t} [T - (U_B + U_C) + W]\, dt = 0 \tag{32}$$

Once the equations of motion are obtained, the viscoelastic damping terms can be introduced by replacing all $E_{C(i)_i}$ and $G_{C(i)}$ with corresponding complex moduli terms. Under harmonic vibration, we can express $E_{C(i)_i}$ and $G_{C(i)}$ as $E_{C(i)} = E'_{C(i)}(1 + i\eta_{C(i)})$ and $G_{C(i)} = G'_{C(i)}(1 + i\eta_{C(i)})$. The loss factors corresponding to extensional and shear deformation of viscoelastic material are assumed to be the same which is a common assumption made with many damping materials. Values of $E'_{C(i)}$ and $G'_{C(i)}$, and $\eta_{C(i)}$ corresponding to a frequency and temperature can be obtained from material data sheets supplied by the manufacturers. The same procedure is followed for introducing the material damping of the composite material. Suppose the lamina has an elastic modulus E_1 along the fiber direction, E_2 along the direction perpendicular to the fiber, and shear modulus G_{12} in xy plane. When the damping of the lamina is considered under harmonic vibration, E_1, E_2, and G_{12} can be replaced by $E_1(1 + i\eta_1)$, $E_2(1 + i\eta_2)$, and $G_{12}(1 + i\eta_{12})$, respectively, where η_1, η_2, and η_{12} correspond to the axial, transverse, and shear loss factors of the lamina material.

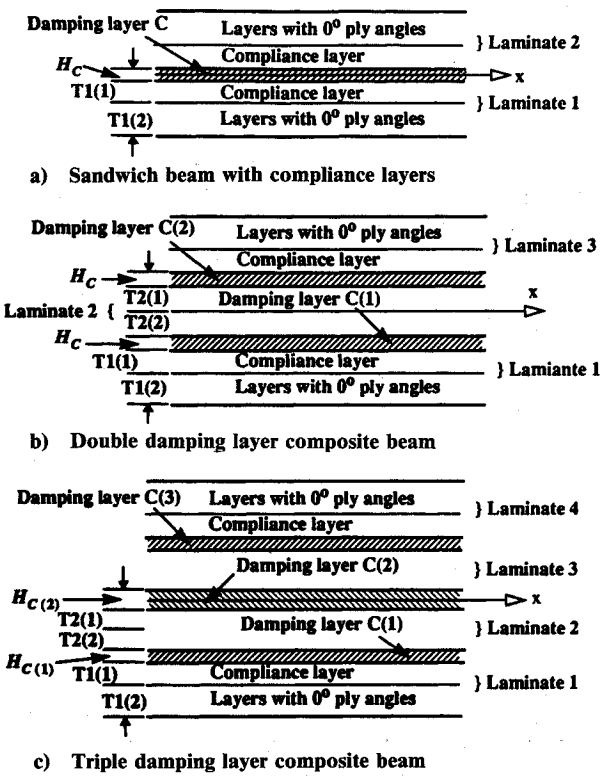

Fig. 2 Dimensions of single, double, and triple damping layer composite beam systems.

Derivation of the Frequency Equation

To find the system modal loss factors and resonance frequencies, we can use the Ritz method. When the simply supported composite beam is under harmonic vibration, the comparison functions for $w(x, t)$, $\gamma_{xz}^{C(i)}$, and $\gamma_{xy}^{(i)}$, $i = 1, \ldots, N$ can be written as

$$w(x, t) = \sum_{k=1}^{\infty} A_k \sin \frac{k\pi x}{L} e^{i\omega t} \tag{33}$$

$$\gamma_{xz}^{C(i)}(x, t) = \sum_{k=1}^{\infty} B_{ik} \cos \frac{k\pi x}{L} e^{i\omega t} \tag{34}$$

$$\gamma_{xy}^{(i)}(x, t) = \sum_{k=1}^{\infty} C_{ik} \sin \frac{k\pi x}{L} e^{i\omega t} \tag{35}$$

where A_k, B_{ik}, and C_{ik}, $i = 1, 2, \ldots, N$, and $k = 1, 2, \ldots,$ are arbitrary constants to be determined. Similar functions for fixed-fixed end conditions are given in Ref. 14.

Considering the first n modes of vibration, we can substitute Eqs. (25) and (29-31) into Eq. (32) by setting $q(x, t) = 0$ and ω to be a complex quantity, i.e., $\omega^2 = \omega_r^2(1 + i\eta)$. The variation of $w(x, t)$, $\gamma_{xz}^{C(i)}$, and $\gamma_{xy}^{(i)}$ will be carried on the arbitrary constants A_n, B_{in}, and C_{in}. After some mathematical manipulation, we obtain the following homogeneous equations:

$$\begin{bmatrix} k_{1,1} - \omega_r^2 M(1 + i\eta) & k_{1,2} & \cdots & k_{1,2n+1} \\ k_{1,2} & k_{2,2} & \cdots & k_{2,2n+1} \\ \cdots & \cdots & \cdots & \cdots \\ \cdots & \cdots & \cdots & \cdots \\ \cdots & \cdots & \cdots & \cdots \\ k_{1,2n+1} & k_{2,2n+1} & \cdots & k_{2n+1,2n+1} \end{bmatrix} \times \begin{bmatrix} A_n \\ B_{1n} \\ \cdots \\ B_{Nn} \\ C_{1n} \\ \cdots \\ C_{Nn} \end{bmatrix} = \begin{bmatrix} 0 \\ 0 \\ \cdots \\ 0 \\ 0 \\ \cdots \\ 0 \end{bmatrix} \tag{36}$$

Setting the determinant of the coefficient matrix of Eq. (36) to zero, we have

$$[k_{1,1} - \omega_r^2 M(1 + i\eta)]\Delta K_{1,1} + \sum_{j=2}^{2N+1} k_{1,j} \Delta K_{1,j} = 0 \tag{37}$$

which is the system frequency equation. From Eq. (37) we get the solutions of ω_r and η in closed form

$$\omega_r = \sqrt{\frac{1}{m} \mathrm{Re}(K_{III})}, \qquad \text{and} \qquad \eta = \frac{\mathrm{Im}(K_{III})}{\mathrm{Re}(K_{III})} \tag{38}$$

where

$$K_{III} = \left[k_{1,1} - \frac{1}{\Delta K_{1,1}} \left(\sum_{j=2}^{2N+1} k_{1,j} \Delta K_{1,j} \right) \right]$$

The terms Re and Im refer to the real and imaginary parts of the complex quantity. The formulas work for the case of $2N$ constraining layers and $2N - 1$ damping layers. If the composite beam consists of $2N$ damping layers and $2N + 1$ constraining layers, the procedure to find ω_r and η is the same except that we will have $(N + 1)$ $\gamma_{xy}^{(i)}$ variables. In this case, $\gamma_{xy}^{(N+1)}$ of the central laminate can be assumed to vary linearly through its thickness. Computer programs have been developed for single, double, and triple damping layer cases to conduct parametric studies.

Numerical Analysis

It is well known that for a single damping layer sandwich beam, the thickness of the damping layer and the material properties (including shear modulus and loss factor) of the viscoelastic material have great effect on the dynamic stiffness and damping capacity of the sandwich beam. For multiple damping layer composite beams, however, in addition to the enumerated factors, the thicknesses of the constraining layers as well as the location of the damping layers will also influence the dynamic stiffness and damping capacity of the beam system. Furthermore, when the constraining layers are laminates, it is expected that the resonance frequency and modal loss factor of the composite beam will also vary with the ply angle of laminas in a certain laminate. This is due to the coupling between the extensional and in-plane shear deformation in the lamina when the composite beam is under bending motion and also due to the change in the beam stiffness with the ply angles of the laminas. The following parametric study shows how the ply angle of each lamina, the damping layer thicknesses, the laminate thicknesses, the location of damping layers in the composite beam, and the operating temperature influence the resonance frequency and modal loss factor of the composite beam system.

Single Damping Layer Composite Beam

The single damping layer sandwich composite beam is shown in Fig. 2a. The inner layers of the base beam (laminate 1) and the constraining beam (laminate 2) close to the damping layer have ply angle θ [i.e., $\theta 1$ (1)] and usually are referred to as compliance layers. The outer layers of the two laminates have 0-deg ply angles and are the dominating layers to maintain the stiffness of the sandwich beam. The first parameter to be studied is the ply angle of the compliance layers.

Numerical results have been generated for a sandwich beam with a layup of $[0_4/\theta_2/d/\theta_2/0_4]$, in which d refers to the damping layer. To compare the present model with Barrett's model,[12] we first generate results using Barrett's input data. Loss factor and normalized resonance frequency of the composite beam vs θ are plotted in Figs. 3a and 3b, respectively.

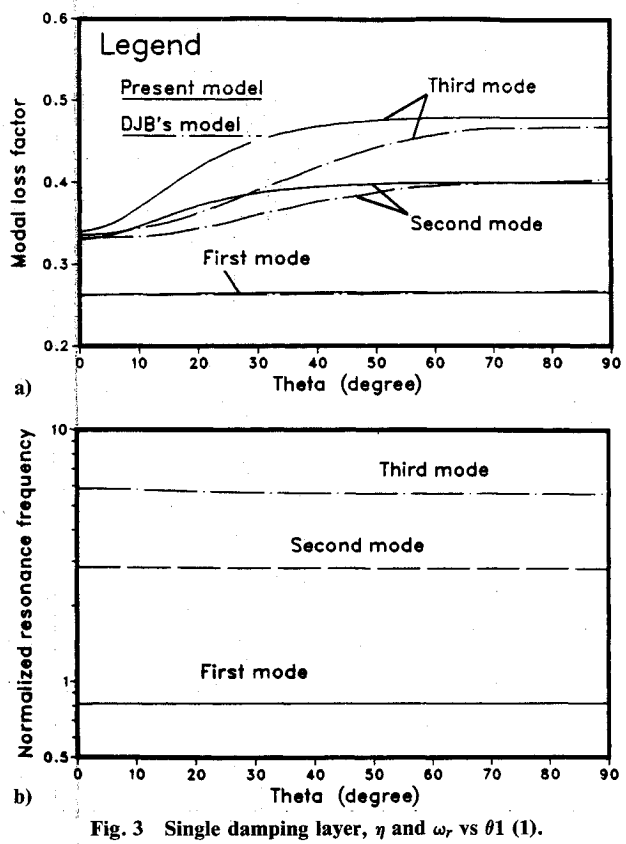

Fig. 3 Single damping layer, η and ω_r vs $\theta 1$ (1).

It can be observed that some minor difference exists between the two models for the second and third mode loss factors. In his model, although Barrett has included the linear variation of the in-plane shear deformation of the two constraining beams through their thicknesses, he neglected the extensional deformation of the damping layer. In addition, Barrett's model was developed for a single damping layer sandwich plate using plate theory, whereas the present formulation is valid for multidamping layers. Another reason for the minor discrepancy between the two results could be that in the present model, some simplifications were made when employing composite laminate theory. For example, we have neglected σ_y of every layer and approximate the extensional deformation of the damping layers to be constant through their thicknesses in calculating the longitudinal strain energy of the damping layers.

Figure 3b shows that the ply angle θ has very little effect on the resonance frequency ω_r. The reason for this is that the plies with angle θ are close to the neutral surface and the total number of these plies are only half of those plies with 0-deg ply angle. Further study of this (results not shown here) has shown that when the number of compliance layers exceed the layers with 0-deg ply angles, the compliance layers will dominate the stiffness of the composite beam; thus increasing the ply angle of the compliance layer will reduce the dynamic stiffness of the sandwich beam. The result of Fig. 3a is obvious. Since the lamina material is much stronger than the damping material, the two constraining beams deform almost independently in flexural vibration. When θ increases, the neutral surfaces of these two beams shift away from the middle surface of the composite beam thus increasing the shear deformation in the central damping layer, which leads to increased damping. Therefore, it can be concluded that increasing the ply angles of the inner layers (compliance layers) can enhance the damping capacity of the sandwich composite beam without reducing the stiffness of the composite beam, if the compliance layers are relatively thinner than the layers with 0-deg ply angle. The normalized resonance frequency in Fig 3b (and all other frequency plots) is normalized with respect to a constant $(\pi/L)^2\sqrt{(H^3E_1)/(12M)}$, where H is the total thickness of the composite beam.

The design of the composite beam to have optimum loss factor for a desired dynamic stiffness requires a knowledge of the variation of dynamic parameters with various structural parameters. We first select the total thickness of the composite beam, the lamina material, the damping material, and the ply angle of the compliance layers. The parameters left to be determined are the damping layer thickness H_C, the thickness $T1(1)$ of compliance layer (or the thickness of the outer layers with 0-deg ply angle), and the operating temperature T. The variation of the maximum loss factor with these three parameters can be shown effectively by the so-called carpet plot. Figures 4a and 4b show two different carpet plots for the composite beam. The total thickness of the composite beam is kept to be 27 layers and each layer has a thickness of 0.127 mm (5 mils). The ply angle $\theta 1(1)$ of the compliance layer is set to be 90 deg. The length of the beam is 0.254 m. The 3M ISD-112 damping material is chosen, and the formulas for calculating the shear storage modulus $G_C'(T, f)$ and material loss factor η_c (T, f) of the damping material corresponding to a frequency f and environmental temperature T can be referred from Ref. 8. The lamina material property data are given by: $E_1 = 148$ GPa, $E_2 = 8.96$ GPa, $G_{12} = 4.48$ GPa, $\rho = 1520$ kg/m^3, $\nu_{12} = 0.35$ (axial Poisson's ratio), $\eta_1 = 0.00128$ (axial loss factor), and $\eta_{12} = 0.011$ (shear loss factor).

In Fig. 4a, $T1(1)$ is varied from one layer (0.127 mm) to 10 layers (12.7 mm) and H_C is varied from one layer to seven layers. When $T1(1)$ is fixed, for a given value of H_C, there will be a unique value of T which yields maximum system loss factor as shown in Fig. 4a. Observation shows that for a fixed H_C, the maximum loss factor does not always increase with $T1(1)$. For example, when $H_C = 0.127$ mm, maximum loss factor increases up to $T1(1) = 5 \times 0.127$ mm, then decreases

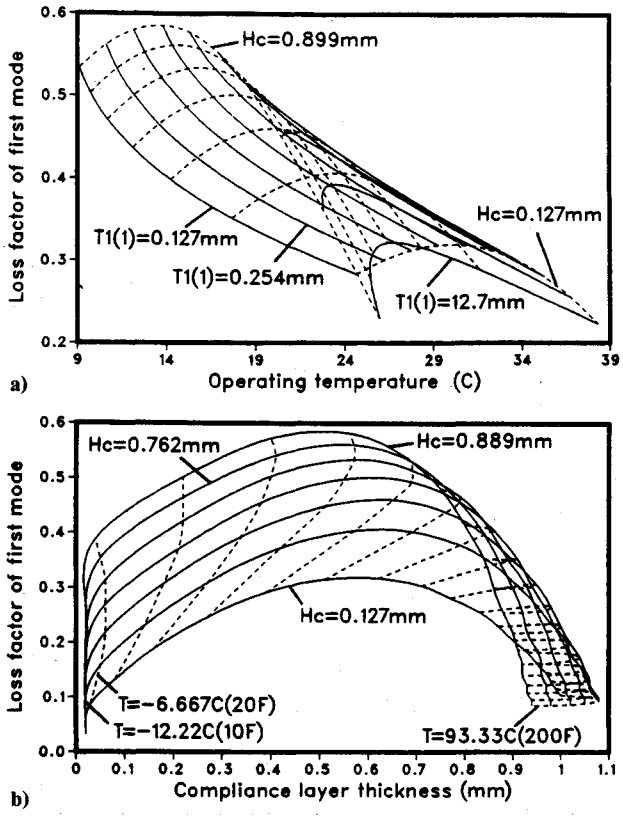

Fig. 4 Carpet plots of optimal η vs T and $T1(1)$, single damping layer.

with further increase in $T1(1)$. To design a sandwich beam having optimal loss factor corresponding to an operating temperature range, we can use these carpet curves in Fig. 4a. For every value of T, there are several combinations of $T1(1)$ and H_C values such that the modal loss factor is maximum. We may also search along the curve H_C = const to find a $T1(1)$ value or vice versa so as to get an optimal loss factor.

Figure 4b in which H_C varies from one layer to seven layers and T varies from -12.22 to 93.33°C is another form of the carpet plot. Here the loss factor is obtained by first fixing the thickness of the damping layer H_C, and operating temperature T, and then changing the thickness of compliance layers $T1(1)$ such that the modal loss factor is maximum. This plot shows that for very low temperature, e.g., $T = -2.22$°C, the thickness of the compliance layers $T1(1)$ to get maximum loss factor for different H_C is almost the same. In fact, if the operating temperature is near or below the glass transition temperature of the damping material, the damping material will become brittle and its modulus will approach the modulus of the lamina material. Then modal loss factor will increase proportionally with H_C. To design a sandwich beam having maximum loss factor corresponding to a fixed operating temperature T, we can search for suitable $T1(1)$ and H_C values along the curve where T = const as shown in Fig. 4b. It should be noted that the given variations presented in the carpet plots are valid only for the damping material chosen; the carpet plot for a different damping material could be entirely different.

Double Damping Layer Composite Beam

Figure 2b shows the double damping layer composite beam. The inner layers of laminates 1 and 3 that are close to the damping layer have thickness $T1(1)$ and ply angle $\theta1(1)$ and are compliance layers. The plies of laminate 2 can also function as compliance layers and have ply angles $\theta2(1)$ or $\theta2(2)$, where $\theta2(1)$ or $\theta2(2)$ correspond to the ply angles of those layers located in the negative or positive x axis. The total thickness of the composite beam is kept to be 32 layers in all the following plots and the length of the beam is set to be 0.254 m as before. The lamina and damping materials are the same as those used in Fig. 4.

Figure 5a shows the case in which only the ply angles $\theta1(1)$ [i.e., theta1(1) in Fig. 5a] of the compliance layers in laminates 1 and 3 are changed and all other layers of the composite beam have 0-deg ply angles. Other input data are $H_C = 0.127$ mm, $T1(1) = T1(2) = 6 \times 0.127$ mm and $T2(1) = T2(2) = 3 \times 0.127$ mm. It can be observed from Fig. 5a that the increase of η with $\theta1(1)$ for the second to fourth mode is significant, but for the first mode η decreases somewhat with $\theta1(1)$.

Figure 5b shows the case in which only the ply angles $\theta2(1)$ [i.e., theta2(1) in Fig. 5b] of the laminate 2 (central laminate) are changed and all other laminas of the composite beam have 0-deg ply angles. Each of the three laminates has 10 layers and the damping layer has a thickness of 0.127 mm. The variation of η with $\theta2(1)$ is similar to that in Fig. 5a. It has also been observed that if laminate 2 is relatively thinner than laminate 1 or 3, η changes very little with $\theta2(1)$. One such numerical example has been shown in Ref. 15. But when laminate 2 is thicker than laminate 1, $\theta2(1)$ will have significant effect on η. For a composite beam with constant thickness, when the number of layers of laminate 2 increases, laminates 1 and 3 will become thinner, which makes laminate 2 to be the dominating laminate. The variation of η and ω_r with the central laminate thickness H_2 is plotted in Figs. 6a and 6b, respectively. Here, $H_C = 0.127$ mm and the ply angles of all of the laminas in the composite are zero. The ω_r-H_2 curve is obvious. When H_2 is very small, the stiffness of the composite beam is determined by the thickness of laminates 1 and 3. On the other hand, when H_2 is much larger than the thickness of laminates 1 and 3, the stiffness of the composite beam will be dominated by laminate 2. The η-H_2 curve shows that lower stiffness corresponds to higher modal loss factor and vice versa; there exists an optimum value of H_2 for maximum loss factor. These two plots clearly show the tradeoffs between the stiffness and the damping capacity that always exist in the design of the composite beam systems incorporating viscoelastic damping materials.

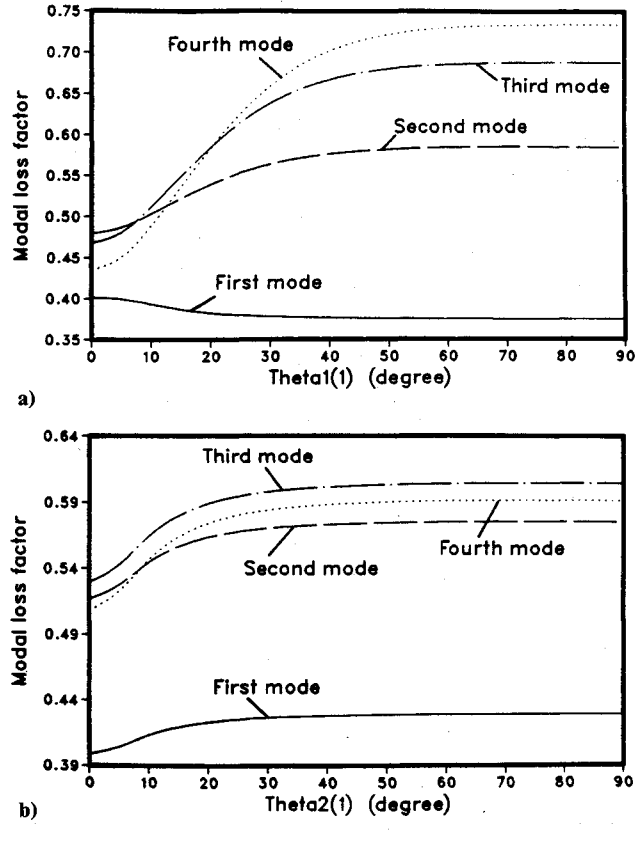

Fig. 5 Double damping layer, η vs $\theta1$ (1) and $\theta2$ (1).

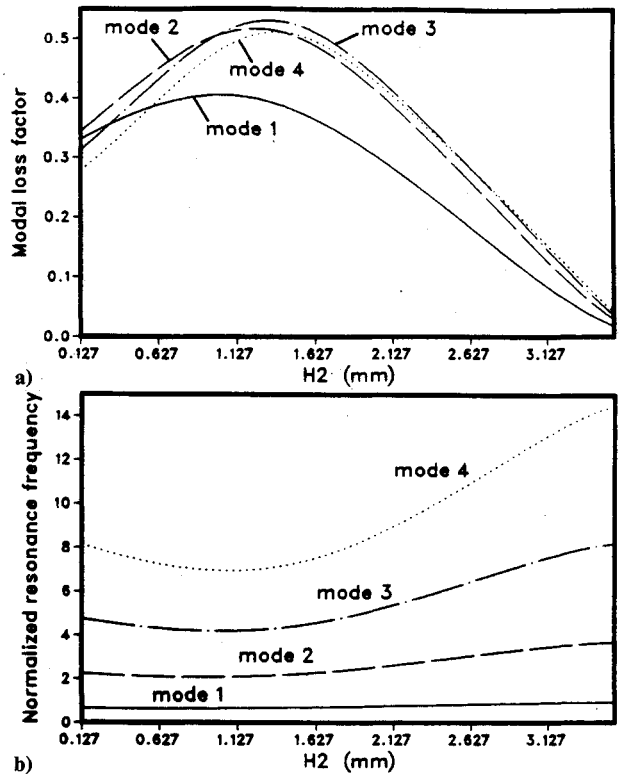

Fig. 6 Double damping layer, η and ω_r vs H_2.

Similar to the sandwich beam case, while designing a double damping layer composite beam, we may fix some parameter such as the total thickness of the composite beam, the ply angle of the laminas, and the thickness of the central beam, and let the other parameters vary. Two carpet plots useful in the design are shown in Figs. 7a and 7b. In Fig. 7a, $T1(1)$ varies from 0.127 mm to 6×0.127 mm and H_C varies from 0.127 mm to 7×0.127 mm. In Fig. 7b, the operating temperature T varies from 4.44°C (40°F) to 48.89°C (120°F) and H_C varies from 0.127 mm to 7×0.127 mm. In both figures, the ply angles of the compliance layers in the two outer laminates are set to be 90 deg which is the best value for obtaining maximum loss factor. All of the other ply angles are kept to be zero. The central beam has four layers. Figure 7a can be used to determine the $T1(1)$ and H_C values for the composite beam to have maximum loss factor corresponding to an operating temperature range. Figure 7b can be employed to find the desired H_C and $T1(1)$ values of the composite beam to have maximum loss factor corresponding to a fixed operating temperature.

Triple Damping Layer Composite Beam

The triple damping layer composite beam is shown in Fig. 2c. In this case, laminates 2 and 3 and the inner layers of laminates 1 and 4 can function as compliance layers. The total thickness of the composite beam is kept to be 31 layers in all of the following plots. The length of the composite beam and the damping and lamina material are the same as before except for the case of two different damping materials.

Figures 8a and 8b show the variation of η with $\theta 1$ (1) for two different cases. Here $\theta 1(1)$ [i.e., theta1(1) in Figs. 8a and 8b] corresponds to the ply orientation of the compliance layers in laminates 1 and 4. All of the other laminas of the composite beam have 0-deg ply angles. In both figures, the damping layers have the same thickness, i.e., $H_{C(1)} = H_{C(2)} = 0.127$ mm. In Fig. 8a, $H_1 = 12.7$ mm, $H_2 = T1(1) = 0.508$ mm, and $T1(2) = 0.762$ mm. In Fig. 8b, $H_1 = H_2 = 0.889$ mm, $T1(1) = 0.254$ mm, and $T1(2) = 0.635$ mm. Numerical data (not plotted here) shows that the ω_r corresponding to Fig. 8a change little with $\theta 1$ (1) for the second to fourth modes, but the ω_r corresponding to Fig. 8b is almost constant with $\theta 1(1)$ for all of the four modes. The reason for this is that there are more plies in the compliance layers for data used in Fig. 8a than for Fig. 8b, which makes both ω_r and η corresponding to data in Fig. 8a to be more sensitive than those of Fig. 8b. It has also been observed that when the thickness of laminates 2 and 3 are larger compared with the thickness of laminate 1 (for example, $H_2 > \frac{1}{2}H_1$), increasing the ply angle of laminates 2 and 3 will significantly increase the modal loss factors of the composite beam.

Figures 9a and 9b plots the variation of η and ω_r with the thickness H_1 of laminate 1, respectively, in which the ply angle of each lamina is zero and $H_{C(1)} = H_{C(2)} = 0.127$ mm. When H_1 is very small, laminates 2 and 3 act as base beams, and laminates 1 and 4 become thin constraining layers. In this situation, the composite beam has maximum dynamic stiffness and very low loss factor. Similarly, when H_2 is very small, laminates 1 and 4 become the dominating beams, and, in this case also, the dynamic stiffness is still high, and the system loss factor is low. There are, however, some values of H_1 and H_2, midway between these extremes that yield maximum loss factor as seen in Fig. 9a.

Figures 10a and 10b show the variation of η and ω_r with the thickness $H_{C(2)}$ of the central damping layer, respectively. The input data are $T1(2) = T2(2) = 0.635$ mm, $T1(1) = T2(1) = 0.254$ mm, $\theta 2(2) = 0$ deg and $\theta 1(1) = \theta 2(1) = 90$ deg. When we fix the thicknesses of the four laminates and increase the thickness of the central damping layer, the thicknesses of the two outer damping layers $C(1)$ and $C(2)$ will be reduced simultaneously since the total thicknesses of the composite beam is kept constant. It can be found from these two figures that increasing $H_{C(2)}$ will improve the damping capacity of the composite beam, but the resonance frequency will be reduced to some extent (especially for higher modes). The same observation has been verified for different ply angles and different combinations of H_1 and H_2.

An added advantage of triple damping layer composite beam is that we may choose different damping materials for $C(1)$ [same as $C(3)$] and $C(2)$, which will enable the composite beam to possess significant damping capacity over a wide

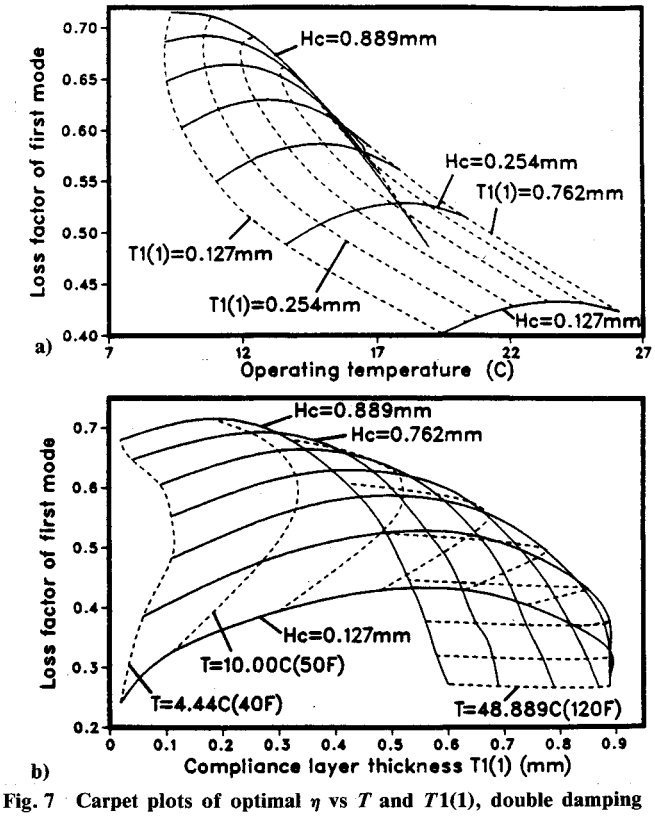

Fig. 7 Carpet plots of optimal η vs T and $T1(1)$, double damping layer.

range of operating temperature. Figure 11a shows the variation of loss factor with operating temperature for two cases when all of the three damping layers are the same. The corresponding resonance frequency-temperature curve for the 3M ISD-113 damping material case is plotted in Fig. 11b. It is clear from Fig. 11 that in this case, the temperature "bandwidth" where the composite beam has maximum loss factor will be relatively narrow. But if we select Soundcoat D material for $C(2)$, and 3M ISD-113 material for $C(1)$ [and $C(3)$], the loss factor and stiffness of the composite beam will be

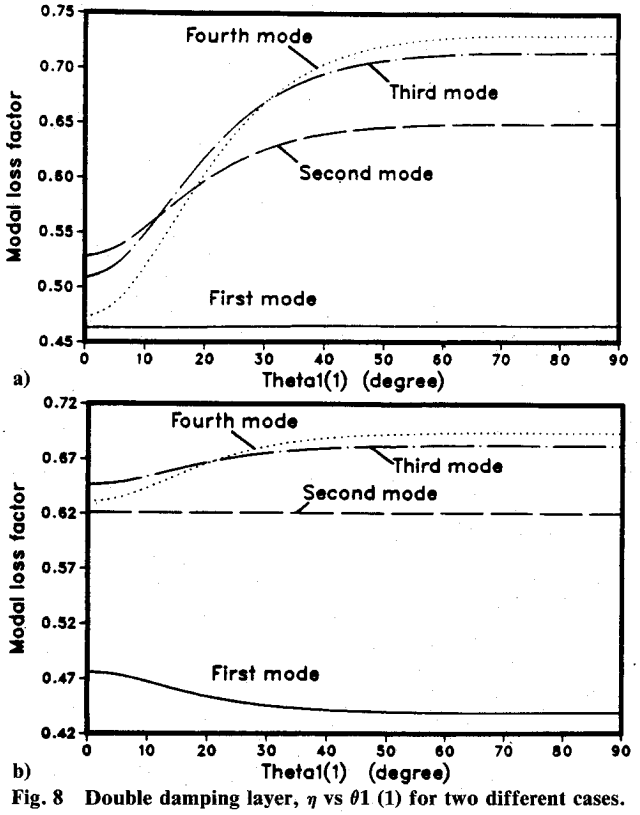

Fig. 8 Double damping layer, η vs $\theta 1$ (1) for two different cases.

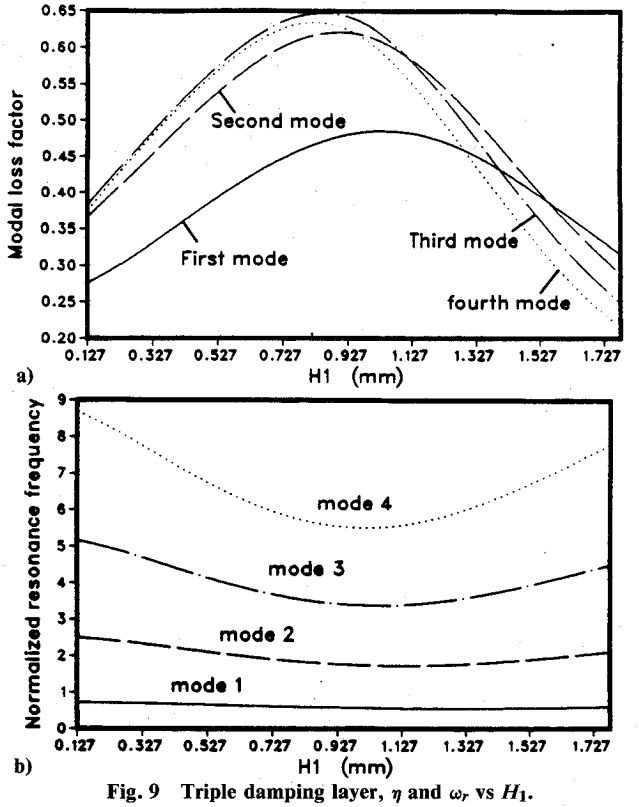

Fig. 9 Triple damping layer, η and ω_r vs H_1.

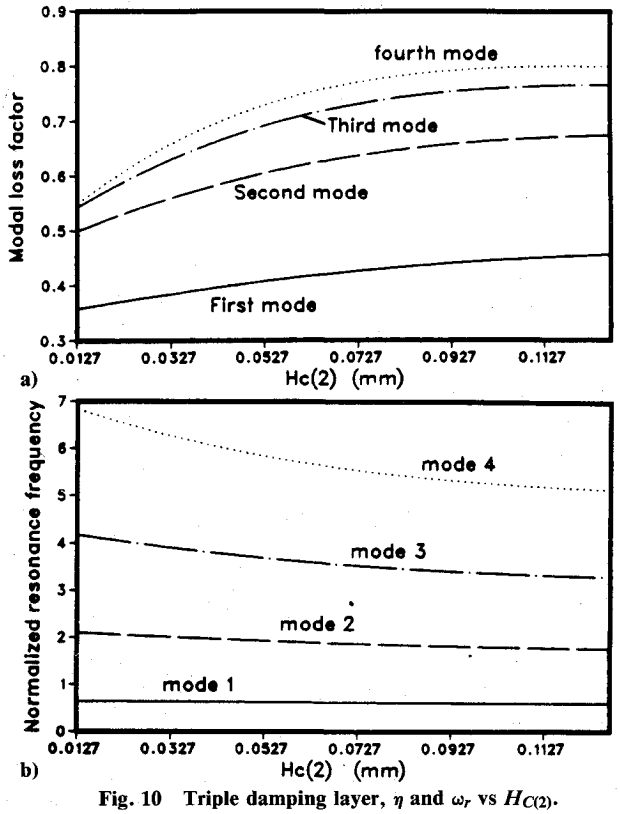

Fig. 10 Triple damping layer, η and ω_r vs $H_{C(2)}$.

greatly improved as shown in Figs. 12a and 12b. The input data for these four plots are the same as those for Fig. 10 except that the thicknesses of the damping layers are fixed to be $H_{C(1)} = H_{C(2)} = 0.127$ mm. Further numerical calculations show that when H_2 is relatively small compared with H_1, the left peak will be higher than the right one for a constant total thickness of the three damping layers, which means that most of the shear deformation occurs in the two outer damping layers instead of the central damping layer. As H_2 increases, the right peak due to the central high temperature damping material will go up while reducing the left peak. When H_2 is larger than H_1, the composite beam becomes much like a sandwich beam with two constraining damping layers on its top and bottom surface. In this case, the central damping layer will undergo more shear deformation than the two constraining damping layers, and thus it is natural that the high temperature damping material will dominate the damping of the composite beam. In addition, it has also been observed that reducing $H_{C(1)}$ and increasing $H_{C(2)}$ will raise the right peak and reduce the left peak, which can be explained by the results shown in Fig. 10. Furthermore, the raising of either peak will raise the overall levels of damping between the two peaks.

Comparison with Experiments

The cocured composite panels were fabricated using 3M SP-319 carbon epoxy prepreg and 3M SJ2015X type 1005 viscoelastic damping material. The prepreg ply has a nominal thickness of 0.14 mm (0.0055 in.) and the damping material has a nominal thickness of 0.127 mm (0.005 in.). A combination of 13 layers of prepreg and viscoelastic material were laid up to from a composite plate with 133.35 mm (5.25 in.) width, 304.80 mm (12 in.) length, and 1.82 mm (0.0715 in.) thickness of uncured composite material. The composite layups were placed into an autoclave and the temperature and pressure cycle recommended by the manufacturer of the prepreg material were followed to cocure the prepreg and viscoelastic materials. Once the large plates are cocured, they are cut into beam samples of 25.4 mm (1 in.) width and 254.0 mm (10 in.) length.

Table 1 Comparison between theoretical and experimental natural frequencies of beam layups with fixed-fixed end conditions

	Mode 1, Hz		Mode 2, Hz		Mode 3, Hz	
Layup	Theory	Experiment	Theory	Experiment	Theory	Experiment
$[0_{13}]$	—	291.2	—	858.9	—	1760
$[0_6/d/0_6]$	309.0	278.7	789.1	780.7	1459	1463
$[0_5/d/0/d/0_5]$	270.2	251.9	687.5	699.7	1192	1296

Table 2 Comparison between predicted and experimental loss factors of beam layups with fixed-fixed end conditions

	Mode 1, %		Mode 2, %		Mode 3, %	
Layup	Theory	Experiment	Theory	Experiment	Theory	Experiment
$[0_{13}]$	—	0.58	—	2.20	—	6.48
$[0_6/d/0_6]$	9.43	6.07	10.13	7.69	10.20	8.93
$[0_5/d/0/d/0_5]$	13.40	8.10	13.47	9.54	13.48	11.43

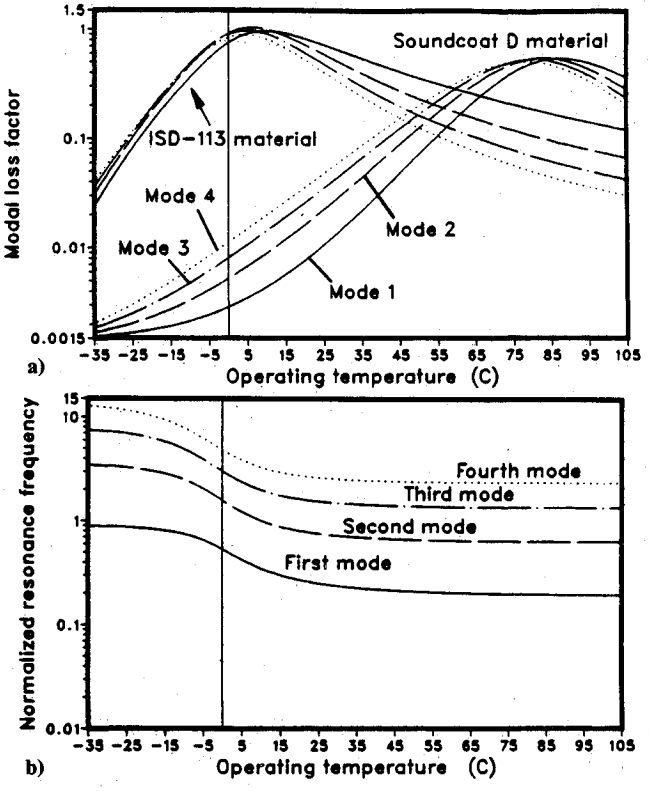

Fig. 11 Triple damping layer, η and ω_r vs T for same damping material.

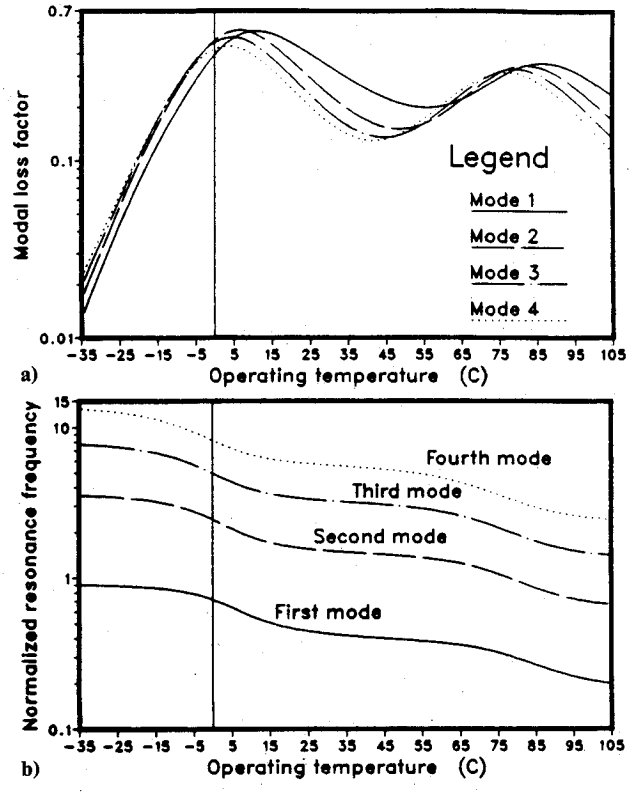

Fig. 12 Triple damping layer, η and ω_r vs T for different damping materials.

The beams were tested using standard experimental modal analysis technique as detailed in Ref. 14. Both cantilever and fixed-fixed type boundary conditions were used. The length of the beam for the fixed-fixed end conditions was 228.6 mm (9.0 in.). A PCB 309A accelerometer was used to measure the vibration response and a PCB 086B80 micro modal hammer was used to excite the structure. The output from the accelerometer and the instrumented hammer were connected to a HP 35660A dynamic signal analyzer to measure the frequency response function. Five averages were taken to obtain the frequency response functions at each point on the beam and care was taken to minimize the noise by monitoring the coherence function between the two channels. The frequency response functions were then transferred to the SMS Star modal software system, and the frequency response functions were curve fit using a polynomial function to obtain the natural frequency and damping ratio for the first three bending modes of the composite beams. Three different modal tests were performed for each beam and the values for natural frequency and damping were averaged to determine mean values for the system.

Tables 1 and 2 show the results of both theoretical and experimental damping ratios and natural frequencies for the first three bending modes for the fixed-fixed end conditions. The $[0_{13}]$ lay up corresponds to the undamped case with no damping material. As can be seen, there is almost an order of increase in the damping capacity of the beam with the addition of one damping layer. There is, however, a decrease in the natural frequency as seen in Table 1 for all of the three modes. The natural frequency of the beam is related to the dynamic stiffness, and this decrease in stiffness is caused by the addition of the damping layer which has a much lower bending stiffness compared with the prepreg material. The addition of two damping layers further increases the damping ratio of the beam but again with some reduction in the dynamic stiffness as evidenced by decrease in system natural frequencies.

From Table 1, it can be seen that the agreement between theory and experiment is good for the natural frequencies for

both single and double damping layer cases. The experimental values for the damping ratio are, however, lower than the values predicted by the theoretical model for both cases (Table 2). The reason for this discrepancy could be attributed to the uncertainties in the estimated material properties of the damping materials. Precise knowledge of damping material shear modulus, loss factor, and their frequency and temperature dependence is important to accurately predict the damping using the theoretical model. In this research, the material data supplied by the manufacturers were used without any verification by independent tests. Furthermore, it has been observed that the predicted values of damping are extremely sensitive to the material properties.

Conclusions

A comprehensive analytical formulation for the vibration and damping analysis of a laminated composite beam with multiple damping layers is described in this paper. The variation of damping capacity and dynamic stiffness of single, double, and triple damping layer composite beams with structural parameters and operating temperature is studied through a number of numerical examples. The parametric design of composite beam systems for optimal damping capacity and desired dynamic stiffness can be obtained through the carpet plots presented in this paper. The following general conclusions have been drawn from the numerical study.

1) For the single damping layer sandwich beam, if the thickness of the compliance layers are small compared with that of the outer layers with 0-deg ply angles, increasing the ply angles of the compliance layers will improve the modal damping capacity without significantly reducing the dynamic stiffness of the sandwich beam.

2) For double and triple damping layer composite beams, the modal damping capacity can be enhanced by increasing the ply angles of the compliance layers in the outer laminates. The same is true for the inner laminates provided the inner laminate thicknesses are close to or larger than the outer laminates.

3) The modal loss factors of the triple damping layer composite beam increase with an increase in the thickness of the central damping layer if the total thickness of the damping layers are kept constant. But the increase in loss factor will lead to a reduction in the dynamic stiffness. Different damping materials can be selected to design a triple damping layer composite system possessing significant damping capacity over a wide operating temperature range.

It should be noted that it is almost impossible to obtain enhanced system damping without some penalties in stiffness. If these penalties can be kept within allowable limits, then laminated cocured panels are extremely effective for passive vibration and noise control. Good agreement between theory and experiment was obtained for the natural frequencies of the system. The theoretical model developed as part of this research can be used in the design and optimization studies of cocured laminated panels incorporating viscoelastic damping materials.

Acknowledgment

The authors would like to acknowledge Roger W. Johnson of the 3M Company who supplied the damping material and composite prepreg for this project.

References

[1]Ross, D., Kerwin, E. M., Jr., and Ungar, E. E., "Damping of Plate Flexural Vibration by Means of Viscoelastic Laminae," *Structural Damping,* edited by J. E. Ruzicka, ASME, New York, 1959, pp. 49–88.

[2]Ditaranto, R. A., "Theory of Vibration Bending for Elastic and Viscoelastic Layered Finite Length Beam," *ASME Journal of Applied Mechanics,* Vol. 78, 1965, pp. 881–886.

[3]Mead, D. J., and Markus, S., "The Forced Vibration of a Three-Layer, Damped Sandwich Beam with Arbitrary Boundary Conditions," *Journal of Sound and Vibration,* Vol. 10, No. 2, 1969, pp. 163–175.

[4]Rao, D. K., "Frequency and Loss Factors of Sandwich Beams under Various Boundary Conditions," *Journal of Mechanical Engineering Science,* Vol. 20, No. 5, Oct. 1978, pp. 271–282.

[5]Miles, R. N., and Reinhall, P. G., "An Analytical Model for the Vibration of Laminated Beams Including the Effects of Both Shear and Thickness Deformation in the Adhesive Layer," *ASME Journal of Vibration, Acoustics, Stress, and Reliability in Design,* Vol. 108, Jan. 1981, pp. 56–64.

[6]He, S., and Rao, M. D., "Vibration Analysis of Adhesively Bonded Lap Joint, Part I: Theory," *Journal of Sound and Vibration,* Vol. 152, No. 3, 1992, pp. 405–416.

[7]Rao, M. D., and He, S., "Vibration Analysis of Adhesively Bonded Lap Joint, Part II: Numerical Solution," *Journal of Sound and Vibration,* Vol. 152, No. 3, 1992, pp. 417–425.

[8]Rao, M. D., and He, S., "Analysis of Natural Frequencies and Modal Loss Factors of Simply Supported Beams with Adhesively Bonded Double-Strap Joints," *Journal of Acoustical Society of America,* Vol. 92, No. 1, July 1992, pp. 268–276.

[9]Miles, R. N., "The Prediction of the Damping Effectiveness of Multiple Constrained Layer Damping Treatments," Acoustical Society of America Meeting, Massachusetts Inst. of Technology, June 1979.

[10]Tujimoto, J., Tamura, T., Todome, K., Tanimoto, T., Suzuki, Y., and Kauchi, K., "Mechanical Properties for CFRP/Damping-Material Laminates," International Conference on Composite Materials, Honolulu, HI, July 1981, pp. 34-D-1–34-D-10.

[11]Mukhopadhyay, A. K., and Kingsbury, H. B., "On the Dynamic Response of A Rectangular Sandwich Plate with Viscoelastic Core and Generally Orthotropic Facings," *Journal of Sound and Vibration,* Vol. 47, No. 3, 1976, pp. 347–358.

[12]Barrett, D. J., "An Anisotropic Laminated Damped Plate Theory," Naval Air Development Center, PA, Rept. NO NADC-90066-60, 1990.

[13]Jones, R. M., *Mechanics of Composite Materials,* Hemisphere, New York, 1975, Sec. 2.6, pp. 47–51.

[14]Gerst, D., Rao, M. D., and He, S., "Damping of Cocured Composite Structures Incorporating Viscoelastic Materials," AMS International Fall Meeting, Chicago, Nov. 1992.

[15]He, S., and Rao, M. D., "Damping of Laminated Composite Beams with Multiple Viscoelastic Layers," *Proceedings of the Second International Congress on Recent Developments in Air and Structure Borne Sound and Vibration,* Auburn Univ., Auburn, AL, March 1992, pp. 265–270.